TiO_2-Derived Titanate Nanotubes by Hydrothermal Process with Acid Treatments and Their Microstructural Evaluation

Atsushi Nakahira,*,†,‡ Takashi Kubo,† and Chiya Numako§

Department of Materials Science, Graduate School of Engineering, Osaka Prefecture University, 1-1 Gakuencho, Naka-ku, Sakai, Osaka 599-8531, Japan, Institute of Materials Research, Osaka Center, Tohoku University, 1-1 Gakuencho, Naka-ku, Sakai, Osaka 599-8531, Japan, and Department of Natural System, Faculty of Integrated Science, The University of Tokushima, 2-24 Shinzocho, Tokushima 770-8502, Japan

ABSTRACT In this study, the effect of post acid treatments with HCl aqueous solutions after the hydrothermal process on the microstructure of TiO_2-derived titanate nanotube was investigated. Especially, the relationship between local structural changes with the HCl treatment and their thermal stability were investigated by X-ray absorption fine structure (XAFS). Consequently, it revealed that the replacement of Na^+ with H^+ (proton exchange) in TiO_2-derived titanate nanotubes was caused by the acid treatment with HCl aqueous solutions and the excess acid treatment led to the disordering. Moreover, it was confirmed that the minor change of TiO_x polyhedra in TiO_2-derived titanate nanotubes was also related with this disordering.

KEYWORDS: titanate • nanotubes • hydrothermal process • acid treatments • microstructure • XAFS

1. INTRODUCTION

For several applications as photocatalysts (1−3), sensors (4), electrochemical capacitors (5), proton conduction (6), and lithium-inserting and ion-exchange materials (7), TiO_2-derived nanotubes are expected to be applicable. Various TiO_2-derived nanotubes with different microstructures have been synthesized by various techniques, such as template method (8, 9), anodic oxidation (10), and hydrothermal method (11). Among them, the hydrothermal treatments of TiO_2 in concentrated aqueous NaOH are fairly simple and enable the production of pure titanate nanotubes at low temperatures (12−16).

It is thought to be very important to control the sodium concentration (Na/Ti) and microstructures for TiO_2-derived titanate nanotubes in order to apply these TiO_2-derived titanate nanotubes prepared by the hydrothermal process to several fields (17, 18). Tsai et al. and Yang et al. have reported that the final pH value of the washing water after the washing process had much effect on the structure of the nanotubes and the layered titanate transformed into a nanotube through $Na^+ \rightarrow H^+$ substitution and eventually transformed into anatase type TiO_2 (19, 20) According to the previous reports (11−20), it has been generally recognized that the nanotubes are identified to be titanate compounds such as $A_2Ti_3O_7$, $A_2Ti_2O_4(OH)_2$/$A_2Ti_2O_5$ $3H_2O$ or lepidocrocite-type $A_xTi_{2-x/4}\square_{x/4}O_4$ (A = Na and/or H, □ = vacancy) and the chemical formula is eventually described as $H_2Ti_nO_{2n+1}$. In their previous studies, the nanotubes having high-porosity prepared by acidic post-treatments washing at pH values of 0−2 had X-ray diffraction (XRD) patterns analogous to that of anatase-type TiO_2 rather than that of the titanate compound. Furthermore, our previous results indicated that TiO_2-derived titanate nanotubes were synthesized by hydrothermal treatment of TiO_2 and the subsequent washing treatments with HCl solution (pH value of 5−13) after the hydrothermal treatments mainly led to the Na/H ion-exchange in the structure for these titanate nanotubes, although some researchers reported that the HCl treatments resulted in the formation of nanotubular structure for these anatase-based nanotubes and titanate-based nanotubes. Thus, the formation mechanism of TiO_2-derived nanotubes during hydrothermal treatment and subsequent washing with HCl solution (i.e., post HCl treatment) are still topics under discussion. In addition, eventually the residue of Na in these nanotubes decreases the photocatalytic ability for obtained nanotbubes. Therefore, the influence of subsequent washing with HCl solution is quite important to understand the mechanism the nanotube formation and post HCl treatments enhance the ability of photocatalytic properties for these nanotubes. Furthermore, upon calcinations of the nanotubes obtained from the acidic post treatment, the samples showed a well-defined anatase phase in their XRD patterns, and also a rutile phase at higher temperatures, reflecting the absence of Na in the nanotubes (20). In contrast, some aggregates with low porosities for nanotubes composed of titanate compound were often obtained after HCl washing at higher pH values, whereas high porosity nanotubes aggregated after washing at pH values of 1−2 (20). Thus, it is anticipated that the control of sodium

* Corresponding author. E-mail: nakahira@mtr.osakafu-u.ac.jp.
Received for review May 20, 2010 and accepted August 5, 2010
† Osaka Prefecture University.
‡ Tohoku University.
§ The University of Tokushima.
DOI: 10.1021/am1004442

ARTICLE

concentration also plays a key role in the local structure and microstructure of nanotubes.

In this paper, the effect of post acid treatments with HCl aqueous solutions on the microstructure and thermal stability of TiO_2-derived titanate nanotubes were investigated by X-ray absorption fine structure (XAFS).

2. EXPERIMENTAL PROCEDURES

TiO_2-derived titanate nanotubes were synthesized through the hydrothermal process. Two grams of anatase-type TiO_2 powder (3 m^2/g, Kojundo Chem. Lab. Co., Ltd., Osaka, Japan) with a particle size of ca. 50 nm as a starting material were used. They were added in 10 M NaOH aqueous solution (20 mL). Then the specimens were treated under a hydrothermal reaction at 383 K for 96 h. The products were separated by filtration and sufficiently washed with deionized water (without HCl aqueous solutions, pH 13.6). After a sufficient washing treatment with deionized water, obtained powders were dried at 323 K for 12 h in an electric oven. Subsequently, as-synthesized TiO_2-derived titanate nanotubes were acid-treated by soaking in 0.1, 1, and 2 M HCl aqueous solutions at room temperature for 2 h. Thereafter, the products were filtered and dried at 323 K for 12 h in an electric oven. TiO_2-derived titanate nanotubes without the acid treatment and acid-treated TiO_2-derived titanate nanotubes were heat-treated at 573 and 973 K for 2 h in air.

Crystalline phase were determined by XRD (RINT 2100, Rigaku Co., Ltd., Tokyo, Japan) with CuKα radiation at 40 kV and 20 mA. XRD profiles were collected between 5 and 60° of 2θ angles. Various microstructural analyses were carried out by using a transmission electron microscopy (TEM, JEM2000FX, JEOL, Tokyo, Japan) with an accelerating voltage of 200 kV and energy-dispersive X-ray (EDX). Nitrogen adsorption isotherms at 77 K were obtained by automatic gas adsorption measurement apparatus (Belsorp 18Plus-SPL, JapanBel, Osaka, Japan) after some pieces of product were pretreated at 403 K for 10 h.

Ti K-edge X-ray absorption near edge structure (XANES) and extended X-ray absorption fine structure (EXAFS) were recorded at room temperature at BL01B1 in the SPring 8 with Japan Synchrotron Radiation Research Institute (ring energy of 8 GeV and stored current of about 100 mV). Ti K-edge XAFS data for this study was collected by transmission mode using the Si (111) double crystal monochromator ($2d = 0.627$ nm). The data were collected by using the ionization chambers filled with gas (I_0 chamber: He/N_2 = 7/3, I chamber: N_2). For XAFS measurements, the samples were prepared as pellets with the thickness varied to obtain a 0.5−1 jump at the Ti K absorption edge. Ti metallic foil was used to carry out for the energy calibration. XANES data were analyzed by subtracting a linear background computed by least-squares fitting from the pre-edge region and normalized. EXAFS data were analyzed by using standard methods. The pre-edge region was subtracted, and then the EXAFS spectra were extracted by fitting the absorption coefficient with a cubic spline method. The Fourier transformation of the k^3-weighted EXAFS oscillation from k space to r space was performed over the range 2.5−11.5 $Å^{-1}$ to obtain radial distribution function (FT-EXAFS). The analysis of EXAFS data was done with the commercial software "REX2000" (Rigaku Co., Ltd., Tokyo, Japan).

3. RESULTS AND DISCUSSION

Figure 1 shows a typical TEM image and EDX result of the product prepared by a hydrothermal treatment of commercial anatase-type TiO_2 at 383 K at 96 h and a subsequent water washing treatment. As shown in Figure 1, the obtained product possessed nanotubular structures with about 10 nm

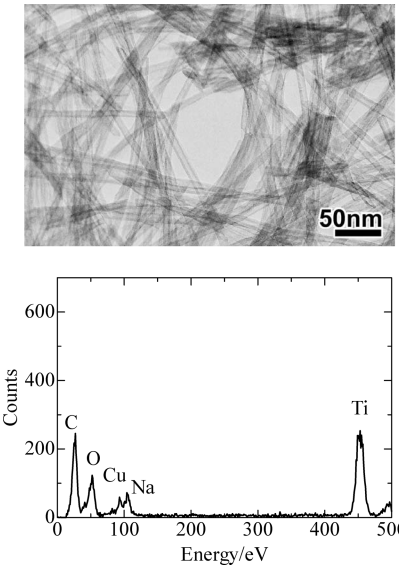

FIGURE 1. TEM image and EDX result of the product prepared by the hydrothermal treatment of commercial anatase-type TiO_2 powder at 383 K for 96 h and the subsequent washing treatment with H_2O.

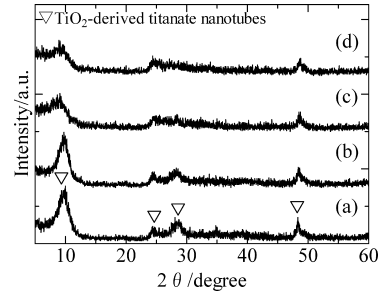

FIGURE 2. XRD patterns of TiO_2-derived titanate nanotubes before and after the acid treatment with HCl aqueous solutions. (a) Before the acid treatment, (b) 0.1 M HCl, (c) 1 M HCl, and (d) 2 M HCl.

in outer diameter and 5 nm in inner diameter and a few hundred nm in length, and they were open-end with several wall layers on both sides. Na/Ti atomic ratio was ca. 0.2 according to EDX analysis. XRD patterns of as-synthesized TiO_2-derived nanotubes and acid-treated TiO_2-derived nanotubes are shown in Figure 2. In the XRD pattern of these samples as shown in Figure 2, the broad reflection peaks were observed at 2θ of approximately 10, 24, 30, 48, and 62°. These peaks have been assigned to the diffraction of titanates.

Figure 3 shows a typical TEM image and EDX results of the TiO_2-derived titanate nanotubes after an acid treatment with 0.1 M HCl aqueous solution. TEM observations indicated that they still possessed nanotubular structures after an acid treatment with 0.1 M HCl aqueous solution. Furthermore, the size and morphology of the nanotubes after HCl treatments were similar to those before HCl treatments. Sodium could not be detected in this sample after an acid treatment with 0.1 M HCl aqueous solution according to EDX analysis, and consequently sodium could be removed from TiO_2-derived titanate nanotubes after an acid treatment. This has been ascribed to the decrease in the Na/Ti ratio of TiO_2-derived titanate nanotubes caused by the replacement of Na^+ with H^+ during the acid treatment with HCl aqueous

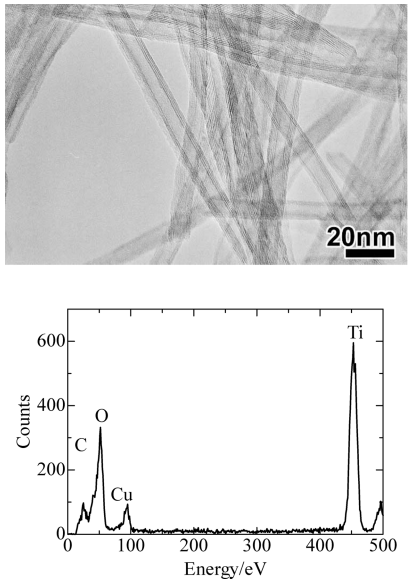

FIGURE 3. TEM image and EDX result for TiO_2-derived nanotubes after the acid treatment with 0.1 M HCl aqueous solutions.

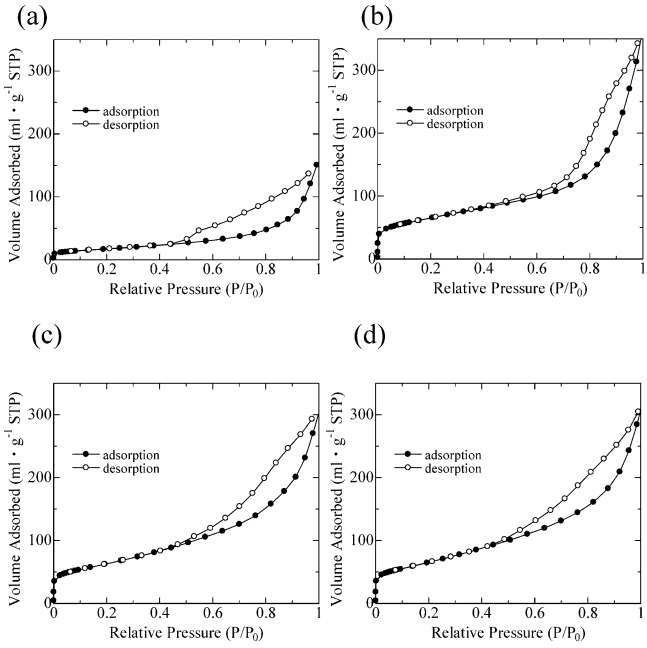

FIGURE 4. Typical adsorption/desorption isotherms of TiO_2-derived titanate nanotubes before and after the acid treatment with HCl aqueous solutions. (a) Before the acid treatment, (b) 0.1 M HCl, (c) 1 M HCl, and (d) 2 M HCl.

solutions. As shown in Figure 2, with an increase in the concentration of HCl aqueous solutions (in particular, in the case of using 1 and 2 M HCl aqueous solutions), there appears to be a corresponding decrease in the intensity of the 30° peak relative to that of 24° peak. According to previous reports (19, 20), it is anticipated that the nanotubes with anatase-phase can be obtained by the further acid treatments with 1 and 2 M HCl aqueous solutions.

Adsorption/desorption isotherms of these samples were also measured by N_2-adsorption. Figure 4 shows the typical isotherms for TiO_2-derived titanate nanotubes before and after HCl treatments. These isotherms exhibit obvious hysteresis behavior, indicating that these TiO_2-derived titanate

Table 1. BET Values of TiO_2-Derived Titanate Nanotubes before and after the Acid Treatment with HCl Aqueous Solutions

	before the acid treatment	after the acid treatment		
		0.1 M HCl	1 M HCl	2 M HCl
BET value ($m^2\ g^{-1}$)	135.2 ± 4.6	219.5 ± 3.4	221.2 ± 4.5	231.7 ± 5.2

nanotubes have mesopores. Values of Brunauer–Emmett–Teller (BET) surface area obtained from N_2-adsorption measurements for these samples were also summarized in Table 1. With an increase in the concentration of HCl aqueous solutions, the surface area value increased, and the BET value of the sample treated with 2 M HCl aqueous solution was ca. 230 m^2/g. After the HCl treatments, the nanotube aggregates should be in a loose configuration, because the porosity was contributed to by the internal space as well as the interstice of the nanotubes, as pointed out by Tsai et al. (20). It is thought that the hysteresis loop of the N_2-adsorption/desorption isotherms supports this argument (Figure 4).

TiO_2-derived titanate nanotubes before and after acid treatments with various HCl concentrations were heated at 573 and 973 K in air atmosphere. Figure 5 shows XRD patterns of these samples after heat-treatments at 573 K (A) and 973 K (B). After a heat-treatment at 973 K, in case of TiO_2-derived titanate nanotubes before the acid treatment with HCl aqueous solutions, diffraction peaks derived from $Na_2Ti_6O_{13}$ were observed. On the other hand, XRD patterns of samples prepared by an acid treatment with a 0.1 M HCl aqueous solution showed that TiO_2-derived titanate nanotubes could be transformed to anatase-type TiO_2, as shown in Figure 5B. Moreover, in the case of excess acid treatments with 1 or 2 M HCl aqueous solutions, diffraction peaks derived from atatase and rutile phases were also observed.

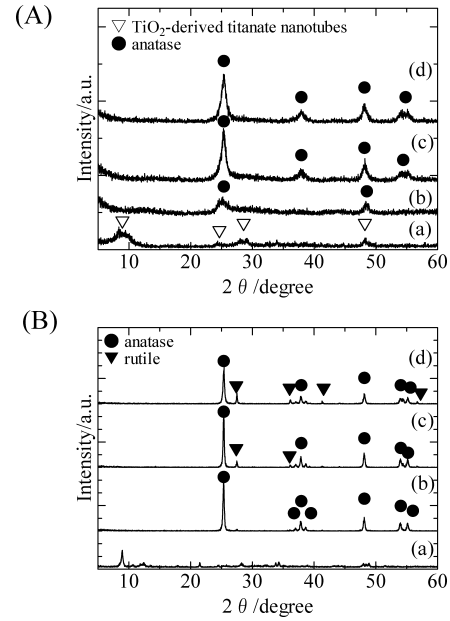

FIGURE 5. XRD patterns of TiO_2-derived titanate nanotubes after the acid treatment with HCl aqueous solutions and subsequently heat-treat at (A) 573 and (B) 973 K: (a) before the acid treatment, (b) 0.1 M HCl, (c) 1 M HCl, and (d) 2 M HCl.

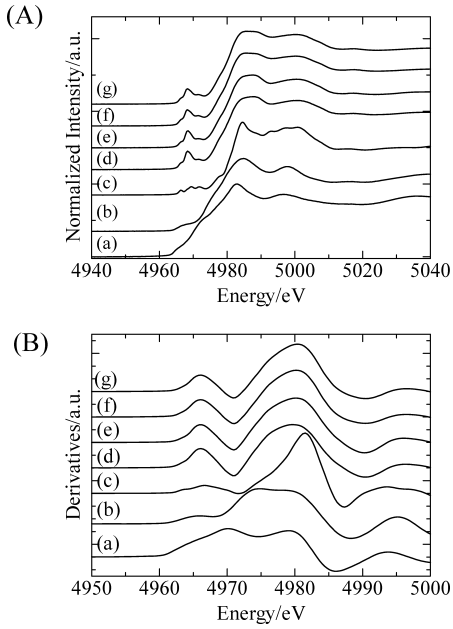

FIGURE 6. (A) Ti K-edge XANES of TiO_2-derived titanate nanotubes before and after the acid treatment with HCl aqueous solutions. (a) TiO, (b) Ti_2O_3, (c) anatase-type TiO_2, (d) before the acid treatment, (e) 0.1 M HCl, (f) 1 M HCl, (g) 2 M HCl. (B) The first derivative of functions of Ti K-edge XANES spectra shown in panel A.

After a heat-treatment at 573 K, as shown in Figure 5A, XRD pattern of TiO_2-derived titanate nanotubes without the HCl treatment was similar to one of this sample before a heat treatment. In contrast, in the case of the sample obtained by an acid treatment with a 0.1 M HCl aqueous solution, the diffraction peak at 25° derived from the (101) diffraction of anatase-type TiO_2 was observed. With an increase in the concentration of HCl aqueous solutions, the anatase-type TiO_2 phase appeared to be the exclusive phase as shown in Figure 5A. These XRD results support the arguments that Na^+ and H^+ in TiO_2-derived titanate nanotubes were exchangeable with the concentration of HCl aqueous solutions. Concurrently, it was obvious that the Na/Ti ratio of TiO_2-derived titanate nanotubes had much effect on the thermal behavior and that Na-containing TiO_2-derived titanate nanotubes were thermally stable.

The effect of the post HCl treatment on the local structure around Ti atom in TiO_2-derived titanate nanotubes was investigated by Ti K-edge XAFS. Figure 6A shows Ti K-edge XANES spectra for TiO_2-derived titanate nanotubes before and after post acid treatments with HCl aqueous solutions. The edge region in the absorption spectra provides much information on the environment geometry and electronic structure of the absorption atom. Figure 6B shows the first derivative regions of Ti K-edge XANES spectra shown in Figure 6A.The edge energy is defined as the energy position corresponding to the peak maximum of the first derivative function. As shown in Figure 6A, the edge energy positions of TiO_2-derived titanate nanotubes prepared by the post HCl treatments were very close to that of TiO_2-derived titanate nanotubes without the HCl treatment. Therefore, the valence number of Ti in TiO_2-derived titanate nanotubes has hardly changed with the post HCl treatment. Here, in Ti K-edge

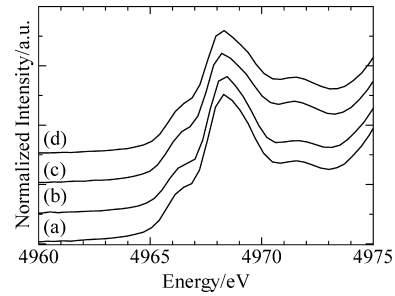

FIGURE 7. Pre-edge of Ti K-edge XANES of TiO_2-derived titanate nanotubes before and after the acid treatment with HCl aqueous solutions. (a) Before the acid treatment, (b) 0.1 M HCl, (c) 1 M HCl, and (d) 2 M HCl.

XANES spectra, the characteristic pre-edge peaks were also observed at 4960−4970 eV. These pre-edge features are widely used to derive information on the coordination environment of Ti atom (21−23). Figure 7 shows the pre-edge of Ti K-edge XANES spectra for TiO_2-derived titanate nanotubes before and after the acid treatments with HCl aqueous solutions. Though their pre-edge features illustrated similar features each other, the pre-edge peak intensity was slightly lower with the post HCl treatments and its intensity was lower as the concentration of the post HCl aqueous solution was higher, which means that local structures around Ti such as the coordination geometry in TiO_2-derived titanate nanotubes have changed with the acid treatment using HCl. The local structural change around Ti was further investigated by Ti K-edge EXAFS.

Figures 8A shows k^3-weighted EXAFS oscillations for TiO_2-derived titanate nanotubes before and after the acid treatment with HCl aqueous solutions and Figure 8B also shows FT-EXAFS for these samples. They represent radial distribution function plots around the Ti atom, and the first peak was indicated as the coordination number corresponding to the Ti−O bond distance. In order to the structural parameters, the curve fitting of the Ti−O shell within the range of 0.6−2 Å was performed by inverse FT. The later each value was obtained from the simulation of the experimental spectrum using the theoretical curves calculated by Mckale et al. (24) The inverse FT of first-shell signal and the best fit are show in Figure 9. In these samples, the agreements between the two curves are quite satisfactory. The parameters obtained by EXAFS analysis are summarized in Table 2. For TiO_2-derived titanate nanotubes without the post HCl treatment, the nearest Ti−O distance and its average coordination number obtained by the curve fitting were 1.92 Å and 5.2, respectively (25, 26). As shown in Figure 8B, though the nearest Ti−O peak geometry and its distance have hardly changed by the acid treatment with HCl aqueous solutions, the peak intensity have changed slightly with the HCl treatment. In fact, values of the nearest Ti−O distance and its average coordination number were also changed as listed in Table 2. These results indicated that TiO_x polyhedra in TiO_2-derived titanate nanotubes have changed due to the post acid treatment with HCl aqueous solutions, and this EXAFS result also agrees with XANES result. Here, although any marked change could not be confirmed in EXAFS oscillations shown in Figure 8A after an acid treatment with

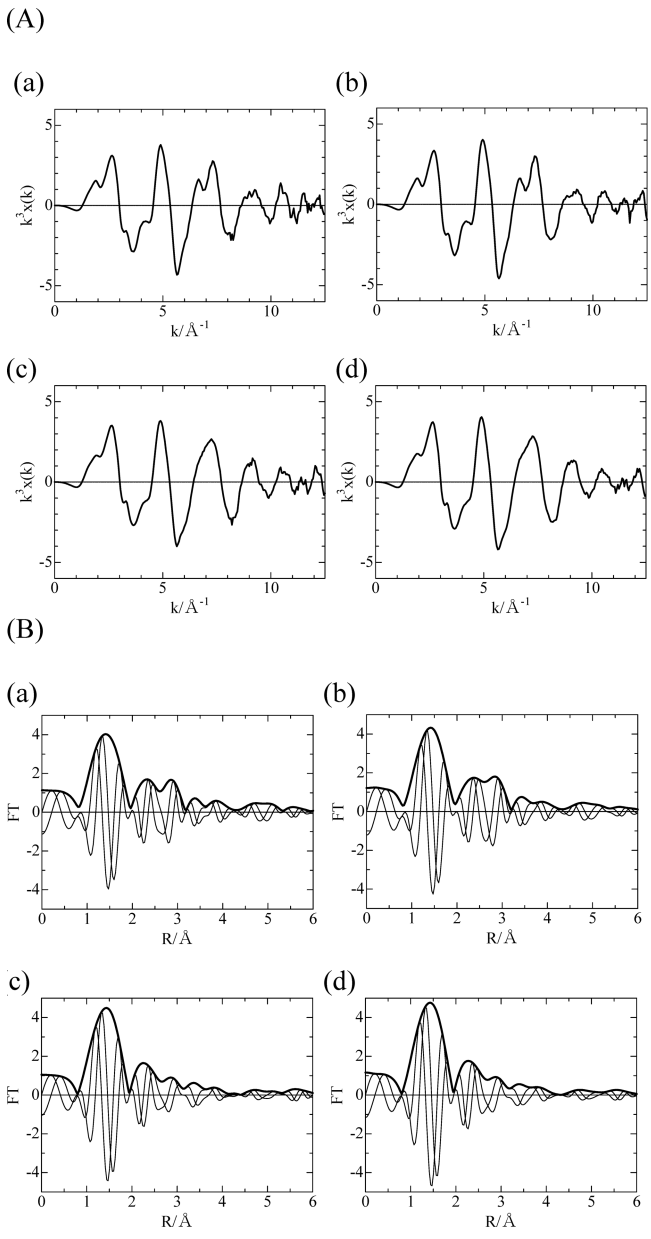

FIGURE 8. (A) k^3-weighted EXAFS oscillations for TiO_2-derived titanate nanotubes before and after the acid treatment with HCl aqueous solutions. (a) before the acid treatment, (b) 0.1 M HCl, (c) 1 M HCl, and (d) 2 M HCl. (B) FT-EXAFS oscillations for TiO_2-derived titanate nanotubes before and after the acid treatment with HCl aqueous solutions. (a) Before the acid treatment, (b) 0.1 M HCl, (c) 1 M HCl, and (d) 2 M HCl.

a 0.1 M HCl aqueous solution, a minor change were observed at k of 6−7 $Å^{-1}$ after excess acid treatment with 1 and 2 M HCl aqueous solutions. Furthermore, the magnitudes of the third peak at R of 2.5 Å got smaller in FT-EXAFS after this excess acid treatment, which means that the third and subsequent ones got structurally disordered in comparison with the sample before and after an acid treatment with a 0.1 M HCl aqueous solution. It is considered that this disordering resulted in the minor change of TiO_x polyhedra in TiO_2-derived titanate nanotubes. This minor structural change in TiO_2-derived titanate nanotubes is now detailed under investigation.

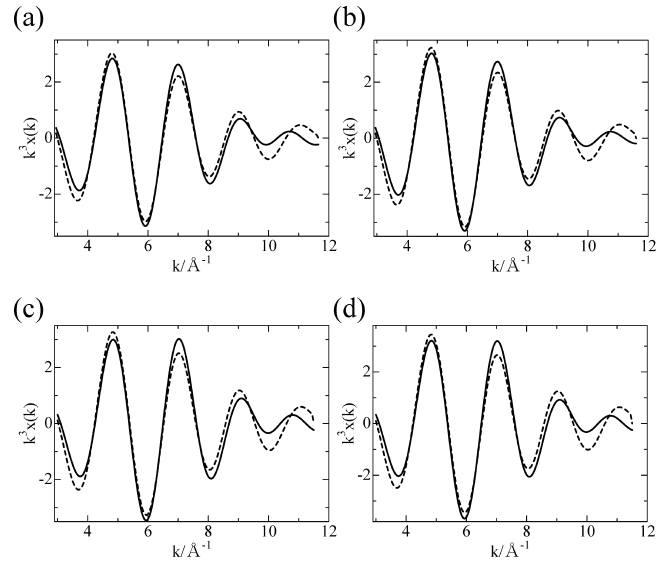

FIGURE 9. Inverse Fourier transforms (full line) and the best fit (dotted line) data for TiO_2-derived titanate nanotubes before and after the acid treatment with HCl aqueous solutions. (a) Before the acid treatment, (b) 0.1 M HCl, (c) 1 M HCl, and (d) 2 M HCl.

Table 2. Nearest Ti−O Distance and Average Coordination Number for TiO_2-Derived Titanate Nanotubes before and after the Acid Treatment with HCl Aqueous Solutions

	nearest Ti−O distance/Å	average coordination number
before the acid treatment	1.92	5.2
0.1 M HCl	1.91	5.1
1 M HCl	1.90	5.2
2 M HCl	1.90	5.1

Thus, it revealed that the replacement of Na^+ with H^+ (proton exchange) in TiO_2-derived titanate nanotubes was caused by the acid treatment with the post HCl aqueous solutions and the excess acid treatment led to the disordering. Moreover, the minor change of TiO_x polyhedra in TiO_2-derived titanate nanotubes was also changed with this disordering. It is speculated that this disordering resulted in the minor change of TiO_x polyhedra in TiO_2-derived titanate nanotubes.

4. CONCLUSIONS

In this study, the effect of post acid treatments with HCl aqueous solutions on the microstructure and thermal stability of TiO_2-derived titanate nanotubes were in detail investigated by TEM, XRD, XAFS, and N_2-adsorption measurements, and the relation between structural changes with the HCl treatment and thermal stability were discussed. With an increase in the concentration of HCl aqueous solutions, the surface area value increased, and the BET value of the sample treated with 2 M HCl aqueous solution was ca. 230 m^2/g. XRD results indicated that the arguments that Na^+ and H^+ in TiO_2-derived titanate nanotubes were exchangeable with the concentration of HCl aqueous solutions. Concurrently, it was obvious that the Na/Ti ratio of TiO_2-derived titanate nanotubes had much effect on the thermal behavior and that Na-containing TiO_2-derived titanate nanotubes were

thermally stable. Ti K-edge XANES and FT-EXAFS showed that the symmetry of the Ti environment in TiO_2-derived titanate nanotubes has hardly changed with the post HCl treatment and that TiO_x polyhedra in TiO_2-derived titanate nanotubes has hardly changed because of these post acid treatments. The third and subsequent ones in FT-EXAFS got structurally disordered in comparison with TiO_2-derived titanate nanotubes without the post acid treatment. Thus, the relation between structural changes with the post HCl treatment and thermal stability was demonstrated by various methods containing XAFS techniques.

Acknowledgment. This work was partly supported by Grant-in-Aid for Scientific Research from Japan Society for the Promotion of Science (20047011). Ti K-edge XAFS measurements were carried out at BL01B1 of SPring8 (2007B1666, 2008A1376). Authors are greatly thankful for the technical support and discussion from JASRI.

REFERENCES AND NOTES

(1) Adachi, M.; Murata, Y.; Harada, M.; Yoshikawa, S. *Chem. Lett.* **2000**, *29*, 942.
(2) Nakahira, A.; Kubo, T.; Yamasaki, Y.; Suzuki, T.; Ikuhara, Y. *Jpn. J. Appl. Phys.* **2005**, *44*, 690.
(3) Kubo, T.; Takeuchi, M.; Matsuoka, M.; Anpo, M.; Nakahira, A. *Catal. Lett.* **2009**, *130*, 28.
(4) Liu, S.; Chen, A. *Langmuir* **2005**, *21*, 8409.
(5) Wang, Y. G.; Zhang, X. G. *J. Electrochem. Soc.* **2005**, *152*, A671.
(6) Thorne, A.; Kruth, A.; Tunstall, D.; Irvine, J. T. S.; Zhou, W. *J. Phys. Chem. B* **2005**, *109*, 5439.
(7) Zhang, H.; Li, G. R.; An, L. P.; Yan, T. Y.; Gao, X. P.; Zhu, H. Y. *J. Phys. Chem. C* **2007**, *111*, 6143.
(8) Hoyer, P. *Langmiur* **1996**, *12*, 1411.
(9) Imai, H.; Takei, Y.; Shimizu, K.; Matsuda, M.; Hirashima, H. *J. Mater. Chem.* **1999**, *9*, 2971.
(10) Gong, D.; Grimes, C. A.; Varghese, O. K.; Hu, W.; Singh, R. S.; Chen, Z.; Dickey, E. C. *J. Mater. Res.* **2001**, *16*, 3331.
(11) Kasuga, T.; Hirashima, M.; Hoson, A.; Sekino, T.; Niihara, K. *Langmuir* **1998**, *14*, 3160.
(12) Du, G. H.; Chen, Q.; Che, R. C.; Yuan, Z. Y.; Peng, L. M. *Appl. Phys. Lett.* **2001**, *79*, 3702.
(13) Sun, X.; Li, Y. *Chem.—Eur. J.* **2003**, *9*, 2229.
(14) Ma, R.; Bando, Y.; Sasaki, T. *Chem. Phys. Lett.* **2003**, *28*, 577.
(15) Nakahira, A.; Kato, W.; Tamai, M.; Isshiki, T.; Nishio, K.; Aritani, H. *J. Mater. Sci.* **2004**, *9*, 4239.
(16) Zhang, M.; Jin, Z.; Zhang, J.; Guo, X.; Yang, J.; Li, W.; Wang, X.; Zhang, Z. *J. Mol. Catal. A* **2004**, *217*, 203.
(17) Yoshida, R.; Suzuki, Y.; Susumu, Y. *Mater. Chem. Phys.* **2005**, *91*, 409.
(18) Poudel, B.; Wang, W. Z.; Dames, C.; Huang, J. Y.; Kunwar, S.; Wang, D. Z.; Banerjee, D.; Chen, G.; Ren, Z. F. *Nanotechnology* **2005**, *16*, 1935.
(19) Yang, J.; Jin, Z.; Wang, X.; Li, W.; Zhang, J.; Zhang, S.; Guo, X.; Zhang, Z. *Dalton Trans.* **2003**, 3898.
(20) Tsai, C. C.; Teng, H. *Chem. Mater.* **2006**, *18*, 367.
(21) Wu, Z. Y.; Ouvard, G.; Gressier, P.; Natoli, C. R. *Phys. Rev. B* **1997**, *55*, 10382.
(22) Chen, L. X.; Rajh, T.; Wang, Z.; Thurnauer, M. C. *J. Phys. Chem. B* **1997**, *101*, 10688.
(23) Hanley, T. L.; Luca, V.; Pickering, I.; Howe, R. F. *J. Phys. Chem. B* **2002**, *106*, 1153.
(24) Mckale, A. G.; Veal, B. W.; Paulikas, A. P.; Chan, S. K.; Knapp, G. S. *J. Am. Chem. Soc.* **1988**, *110*, 3763.
(25) Kubo, T.; Nakahira, A. *J. Phys. Chem. C* **2008**, *112*, 1658.
(26) Kubo, T.; Yamasaki, Y.; Nakahira, A. *J. Mater. Res.* **2007**, *22*, 1286.

AM1004442